COMPARATIVE STUDY OF THE CRYOSURGICAL PROCESSES WITH TWO DIFFERENT CRYOSURGICAL SYSTEMS: THE ENDOCARE CRYOPROBE SYSTEM *VERSUS* THE NOVEL COMBINED CRYOSURGERY AND HYPERTHERMIA SYSTEM

G. ZHAO[†,*], D.W. LUO[‡], Z.F. LIU[§] and D.Y. GAO[¶]

† *Department of Modern Mechanics, University of Science and Technology of China, Hefei 230027, P.R. China*
ZhaoG@ustc.edu.cn

‡ *Department of Chemical Engineering, Texas A & M University, College Station, TX, 77840, USA*

§ *Department of Thermal Science and Energy Engineering, University of Science and Technology of China, Hefei 230027, P.R. China*

¶ *Department of Mechanical Engineering, University of Washington, Seattle, WA 98195, USA*

***Abstract*— A numerical model was developed to study heat transfer process during freezing of biological tumors. Two different cryosurgical systems, Endocare cryoprobe and novel combined cryosurgery and hyperthermia system, were investigated using the multidimensional, finite element method (FED) developed in Ansys (V7.0) by us recently. The tissues were modeled as nonideal materials, the thermophysical properties of which were temperature dependent. The enthalpy method was applied to solve the highly nonlinear problem. It was found that for the same initial/boundary conditions and the same target tissues, the novel combined cryosurgery and hyperthermia system could supply the target tissue an approximate cooling rate, a much lower minimal temperature, a much greater warming rate, and a much greater thermal gradient as compared with the Endocare cryoprobe system. The numerical simulation results indicated that the novel combined cryosurgery and hyperthermia system could provide an excellent curative effect in the corresponding cryotherapy.**

***Keywords*— FED, heat transfer, cryosurgery, cryoprobe, Ansys**

I. INTRODUCTION

Cryosurgery has been recently accepted as a treatment option for eradicating undesirable tissues, especially tumor tissues, due to its minimal invasiveness and little hospitalization needs. Since 1845, a partly frozen saline solution (at about -22°C) was used to treat skin cancer tumors by James Arnott, it has been a known surgery treatment (Gage, 1992; Rabin and Stahovich, 2003). And it has become a well-established method for the ablation of benign and malignant lesions since the mid-1960s (Gage, 2004; Deng and Liu, 2005). Cryosurgery is an effective treatment for both surface tissues and internal organs, and the minimally invasive cryoprobe known widely today is suitable for the latter. The first cryoprobe was designed to treat brain tumors and the part of the brain associated with Parkinson's disease (Lee, 1967; Rabin and Stahovich, 2003). Although the application of cryosurgery for treatment of renal, cerebral, adrenal and breast cancers is under way, the treatment modality is most commonly used for the eradication of prostate and liver tumors (Rewcastle *et al.*, 1998). And recent improvements in imaging techniques, such as magnetic resonance imaging (MRI), computerized tomography (CT), and electrical impedance tomography (EIT), have stimulated the spread and popularity of cryosurgery (Baust and Gage, 2004).

In a typical cryosurgery process, the undesired tissues will undergo liquid-solid and reverse phase transformation in the freezing/thawing region, where the tissues will be injured or destroyed by several mechanisms, such as "solution injury", injury caused by "intracellular ice formation (IIF)", the re-crystallization of intracellular ice, thermal stress, (Zhang *et al.*, 2000; Mazur *et al.*, 1972; Zhao *et al.*, 2006b; Zhao *et al.*, 2007). Successful cryosurgery means maximal destruction of undesired tissues by freeze-thaw cycle, but the effect of cryosurgery is often influenced by the thermal history experienced by the tissues, which includes the cooling rate, the thawing rate, the minimal temperature, the freeze-thaw cycles, (Smith and Fraser, 1974; Gage *et al.*, 1985; Hua and Ren, 1994; Miller and Mazur, 1976; Gage *et al.*, 1982; Tackenberg, 1990; Rand *et al.*, 1985). A 'critical isothermal protocol', which assumes that complete necrosis occurs only in regions where have been embraced by a certain isothermal surface, is often regarded as a standard clinical procedure (Rewcastle *et al.*, 1998). However, there is some variance in literatures regarding the absolute value of this critical temperature. For example, the critical temperatures listed by Gage and Baust in two recent reviews range from -2 (osteocytes, bone, dog) to -70°C (adenocarcinoma, rat) (Gage and Baust, 1998; Gage, 2004). So the critical temperature is likely to be tissue dependent, and this assumption has some biological basis.

The *in vivo* growth of the iceballs could be commonly monitored with real-time two-dimensional ultrasound. Since ultrasound is almost 100% reflected at the ice interface, the imaging modality enables the iceball edge to be observed clearly while the three-dimensional

geometry of the iceball and the unfrozen tissue completely enveloped by the frozen tissue are both impossible to be imaged (Sandison *et al.*, 1998; Rewcastle *et al.*, 1998). Although an MR or CT imaging modality could be chosen to visualize three-dimensional geometry of the iceball (Saliken *et al.*, 1996; Hamer *et al.*, 1995), none of these above mentioned imaging modalities could visualize the internal thermal field of the iceball, the surgeon remains blind to the location of the critical isotherm(Rewcastle *et al.*, 1998).

In contrast to the imaging technology, numerical simulation technique can be used to obtain transient thermal field inside the target tissues as long as the boundary, initial conditions and the thermal properties of the target are accurately set. By solving the multidimensional heat transfer problem during cryosurgery numerically, it is possible for the surgeon to control and optimize the protocol of the cryosurgery. The numerical approaches to the multidimensional freezing/thawing problems during cryosurgery may generally be divided into two categories, the finite difference method (FDM) and the finite element method (FEM). Rabin and Shitzer (1998) used FDM to predict the freezing front propagations around the spherical cryoprobe in soft biological tissues, including the influences of the length and diameter. Deng and Liu (2005) used the same method to study the effect of pre-injection solutions with high thermal conductivity or low latent heat into the target tissues before cryosurgery. Zhang *et al.* (2005) and Zhang *et al.* (2000) carried out finite element analysis (FEA) of the freeze-thaw processes around the cryoprobe. Compared to FDM, FEM is more suitable for irregular boundaries, and this is often the case in tumor tissues. For example, Zhang *et al.* (2005) used FEA to simulate the heat transfer in prostate cancer cryosurgery, where the three-dimensional geometric model was directly generated from the MRI images of a real prostate. In the work of Zhang *et al.* (2000) the heat source term caused by the blood perfusion and the metabolic heat generation was not considered, and the influence of the thermal insulation part of the cryoprobe was not referred to. However, the *in vitro* experiments agreed well with the theoretical predictions when the heat source terms were both omitted (Zhang *et al.* ,2000). Although the heat source term was included in the theoretical study of Deng and Liu (2005) due to the limitation of the FDM, certain simplifications were assumed (the cylindrical cryoprobe and the tumor domain were both approximated as cubes, and the temperature of the cryoprobe tip was fixed at -196°C).

Based on the recently realized fact that freezing immediately followed by a rapid and strong heating of the target tissues would dramatically improve the destructive effect (Zhang and Liu, 2002; Liu *et al.*, 2001), a new minimally invasive cryoprobe system with powerful heating feature was developed and described in detail elsewhere (Liu *et al.*, 2004), the liquid nitrogen or high-temperature vapor can be selectively and alternatively transferred through the rube to the tumor to control its temperature varying between -175 to 75°C. Due to the shortdated existence of such combined cryosurgery and hyperthermia system, little attention has been paid to the freezing/thawing behaviors of the biological tissue subject to it (Deng and Liu, 2004b; Zhao *et al.*, 2006a). Deng and Liu (2004b) used FDM to simulate the freezing and heating problems for such system, while the cylindrical probe was approximated by a cube again, and the temperature of the surface of the probe was fixed at 80°C and -196°C to simulate the effect of heating and freezing stage of the probe, the critical isothermal surface was not discussed.

In this study, the multidimensional transient heat transfer problems involving freezing and heating of biological tissues during the cryosurgical processes with the Endocare cryoproble system and the novel combined cryosurgery and hyperthermia system were comparatively investigated (the two systems will be called as “System Endocare” and “System CH” for brevity). FEM was used to solve the enthalpy formed classical bioheat equation put forward by Pennes (1998).

The objectives of this paper are: (a) To comparatively study the cooling/heating features, including the transient thermal and thermal gradient fields, of the above mentioned two kinds of cryoprobe systems during the typical cryosurgical processes; (c) To comparatively study the propagations of the freezing front and the critical isothermal surface, and to evaluate the effectively destroyed regions of such cryoprobes during the typical freezing/thawing processes; (d) To fully investigate the new heat transfer features of System CH during cryosurgery compared to System Endocare.

II. METHODOLOGY

A. Mathematical Formulation

The classical bioheat equation put forward by Pennes (1998) has been commonly used to describe the heat transfer in freezing of biological tissues, which can be written as its enthalpy form:

$$\frac{\partial(\rho h)}{\partial t} = \nabla\cdot(k\nabla T) + \rho_b c_b \dot{\omega}_b (T_b - T) + \dot{q}_{met}, \qquad (1)$$

where ρ is the density of the tissue, and ρ_b is the density of the blood; h, enthalpy; t, time; $\dot{\omega}_b$, the blood perfusion rate (ml·s^{-1}·ml^{-1}, the volumetric blood flow rate per unit volume of tissue); T_b, the blood temperature and T, the tissue temperature; c_b, the specific heat capacity of blood; $\dot{q}_{met}$, the metabolic heat generation (w·m^{-3}). The second and the third terms of Eq. (1) are the heat source contributions from blood perfusion and metabolic heat generation respectively. The sum of the two terms is the total heat source, marked as “Q”. Equation (1) is based on the assumption that blood in the biological tissue is supplied with an isotropic capillary network and it enters the tissue at the blood temperature of the major supplying artery and leaves the tissue at the tissue’s temperature (Zhang *et al.*, 2005).

For biological tissues, the phase transformation often

occurs over a temperature range (T_{ml} , T_{ms} , the upper and lower limit of the phase change temperature), the enthalpy is related to the tissue temperature by followings:

$$\rho h = \begin{cases} c_s\rho_s\left(T-T_r\right), & T < T_{ms} \\ c_s\rho_s\left(T_{ms}-T_r\right)+\dfrac{T-T_{ms}}{T_{ml}-T_{ms}}\cdot L, & T_{ms} \le T \le T_{ml} \\ c_s\rho_s\left(T_{ms}-T_r\right)+L+c_l\rho_l\left(T-T_{ml}\right), & T > T_{ml} \end{cases} \quad (2)$$

where, subscripts *s*, *l*, *ms*, *ml* refer to the solid, liquid state, the lower and upper limit of the phase transformation; *L*, latent heat; T_r (=-175°C), the reference temperature.

From the above equations, it can be seen that, in the enthalpy method, enthalpy and temperature are both regarded as independent variables. Thus a uniform heat conduction equation is available covering all times across the phase transformation range. The following assumptions were made during the solution of the mathematical model: (i) The undesirable tissues (ordinary tumor tissues) which need to be eradicated and the surrounding normal tissues are assumed to have the same thermal properties. This is due to the lack of experimental data for normal and tumor tissues over the studied temperature range (Zhang *et al.*, 2005); (ii) The phase transformation of the biological tissues during cryosurgery occurs over certain temperature range, T_{ml} (-1°C) and T_{ms} (-8°C) (Wessling and Blackshear, 1973); (iii) The density of the frozen and unfrozen tissues are assumed to be the same, the volume changes caused by the phase transformation are completely omitted (Deng and Liu, 2005; Zhang *et al.*, 2005); (iv) The metabolic heat generation and the blood perfusion are valid only before the phase transformation. Once the tissues are partially frozen, the entire heat source term is omitted (Deng and Liu, 2005, 2004a, b); (v) The thermal conductivities are two different constants before and after the phase transformation, and change along with the temperature during phase change. (vi) The temperature profiles along the conductive parts of the probes are assumed to be uniform for both the new and the Endocare systems, for no such experimental data files are available.

B. Boundary and Initial Conditions

The schematic presentation of the target tissue and the cryoprobe is depicted in Fig. 1, in which the cryoprobe and the tissue are represented as two cylinders with the same axis. *x* denotes the radius of the cryoprobe and the tissue, and *y* denotes the height of certain point inside the tissue cylinder. R_{x} donates the maximal distance from the symmetrical axis to the freezing front in *x*-direction. Path-*x* and Path-*y* are the two typical paths selected for the study of temperature distributions in *x*-direction and *y*-direction crossing the farthest point of the freezing front in that direction separately. The inserted length of the thermal insulation domain of the cryoprobe is one third its active domain.

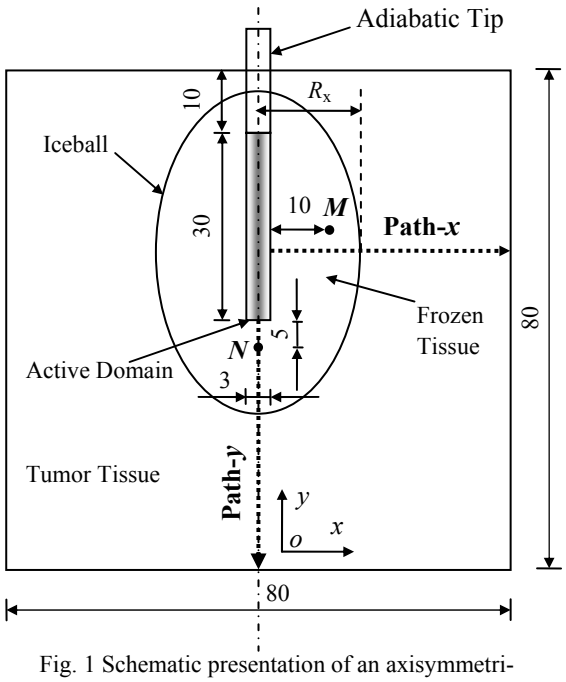

Fig. 1 Schematic presentation of an axisymmetrical freezing problem around a cylindrical cryoprobe (unit: mm).

The typical temperature profiles of the active surfaces ($T_{\mathrm{probe(t)}}$) of System Endocare and System CH are described as followings:

(a) For System Endocare, as yet the only commercially available cryoprobe system with both strong freezing and quick heating capability (Liu *et al.*, 2004) , that is: (i) firstly freezing from 37 to -140°C at a constant cooling rate (about 34°C/min) in 310s; (ii) then holding at -140°C from 310 to 1500s; (iii) and after that heating from -140 to 20°C from 1500 to 1718s at a constant warming rate (about 44°C/min); (iv) at last, holding at 20°C from 1718s to 3000s.

(b) For System CH, first reported by Liu *et al.* (2004) elsewhere, that is: (i) firstly freezing from 37 to -175°C at a constant cooling rate (about 31°C/min) in 409s; (ii) then holding at -175°C from 409 to 1500s; (iii) and after that heating from -175 to 75°C from 1500 to 1562s at a constant warming rate (about 240°C/min); (iv) at last, holding at 75°C from 1562 to 3000s.

It should be pointed out that, the above temperature profiles of the cryoprobes were designed according to the real experimental data of such cryoprobes on the rabbit tissues or organs (Liu *et al.*, 2004). That is to say, the temperature *versus* time profiles were obtained with the full power running cryoprobe systems, which were not merely the user set cryosurgical programs but reflected the intrinsic features of such systems.

The right half of the longitudinal cross-section of the tumor tissue cylinder was selected as the modeling geometry, since the problem is axisymmetrical. The boundary conditions of the irregular calculation domain were defined as follows:

i) $-k\dfrac{\partial T}{\partial y}=h_{air}\left(T_{air}-T\right)$

at $0.0015\le x\le 0.04,\quad y=0.08;$

ii) $T=T_c$

at $x=0.04, 0<y<0.08$ or $0\le x\le 0.04, y=0;$

iii) $-k\dfrac{\partial T}{\partial x}=0$ at $x=0, 0<y<0.04$

or $x=0.0015, 0.07<y<0.08;$

iv) $T=T_{probe}(t)$ at $0\le x\le 0.0015, y=0.04$

or $x=0.0015, 0.04<y\le 0.07;$

where T_c (=37°C) and T_{air} (=20°C) are the temperatures of the body core and the surrounding air, respectively; h_{air} (=10w·m^{-2}·°C^{-1}) is the convective heat transfer coefficient between the environment and the skin surface. The region far from the cryoprobe was assumed to be kept at T_c. Ideally, the tissue surface adhered to the surface of the cryoprobe was assumed to be at the temperature $T_{probe}(t)$. The thermal insulation part was assumed to be completely thermally insulated.

The initial temperature field in the tissue was simplified as $T_0(x,y)=T_c$ for all x, y.

C. Geometry Meshing and Convergence Check

In the GUI of Ansys 7.0, the "Defined Element Types" was set to be "PLANE55", and "Element behavior" was set to be "Axisymmetric". The smart mesh method was used to produce high quality grids of the irregular geometry of the tissue. The type of the element was selected as "triangle", and the "smart,1" command was used to produce the finest grids of the default mesh method, then all the elements were refined for a second time, and after that the grids were checked again to find out the elements that need to be refined and refined them, this check and refine work were repeated until there were no elements that need to be refined further. The final meshed geometry of half of the longitudinal cross-section of the tumor tissue cylinder included 2857 nodes.

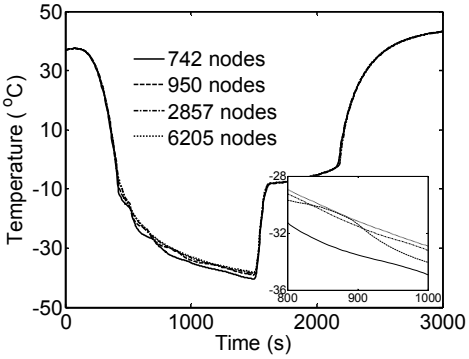

Fig. 2 Convergence check of the numerical solution (thermal histories of point M under different nodes).

In order to evaluate the quality of the meshed grids, two other coarser and one finer meshed grids were compared in Fig. 2. The meshing method used in this paper corresponds to 2857 nodes. From Fig. 2, it can be seen that the two coarser meshed grids can not supply the smooth thermal histories of the typical point (point M, as shown in Fig. 1), while the grids used in this study and the finer meshed grids can both supply the better thermal histories of the point. Besides, the meshed grids used in this study gave out a very close curve to that of the finer meshed grids. So the grids used in this study were fine enough for the accurate solution of this problem.

D. Thermophysical Properties

Typical tissue thermal properties were selected according to the values of the soft biological tissues gave by Shitzer and Eberhart (1985) and Rabin and Shitzer (1998), as shown in Table 1.

The blood perfusion related term, $\dot{w}_b C_b$, was assumed to be 10 kW·m^{-3}·°C^{-1}, as its value varys between 0 to 40 kW·m^{-3}·°C^{-1} for different physiological conditions.

E. Numerical Solver

In the GUI of Ansys7.0, the "type of analysis" was set to be "transient", the "line search" in the "nonlinear options" was triggered on, and the "maximum number of iterations" of "equilibrium iterations" was set to be 200. Due to the fact that phase transition is included in the problem, the time step must be small enough, and so the "time step size" was set to be 0.01, the "minimum time step" was set to be 0.01, the "maximum time step" was set to be 5. Then the time step size may be selected automatically between 0.01 and 5 by the solver.

The variations of thermal properties and blood perfusion with temperature made the energy equation highly nonlinear. Ansys used the "Newmark Algorithm" for time integration, "Prog Chosen" for the "DOF solution predictor". The "Program chosen solver" was used to solve the equation.

During the simulation, the convergence monitor for each DOF, such as temperature, heat flow, etc, was calculated. The convergence monitor for each variable ϕ was defined as following:

$$\text{convergence monitor} = \left(\sum_{i=1}^{n}\left|\phi_i^k-\phi_i^{k-1}\right|\right)\Big/\left(\sum_{i=1}^{n}\left|\phi_i^k\right|\right)$$

In this study, the criterion of convergence for heat flow was set to be 10^{-3}.

Table 1. Thermal properties of soft biological tissues

Parameter	Unit	Value
Upper limit of phase transition	°C	-1
Lower limit of phase transition	°C	-8
Blood temperature	°C	37
Thermal conductivity of unfrozen	w·m^{-1}·°C^{-1}	0.5
Thermal conductivity of frozen	w·m^{-1}·°C^{-1}	2.0
Specific heat of unfrozen tissue	MJ·m^{-3}·°C^{-1}	3.6
Specific heat of frozen tissue	MJ·m^{-3}·°C^{-1}	1.8
Latent heat	MJ·m^{-3}	250
Blood perfusion rate, $\dot{w}_b$	ml·s^{-1}·ml	≤0.011
Metabolic heat generation	kW·m^{-3}	33.8

F. Model verification

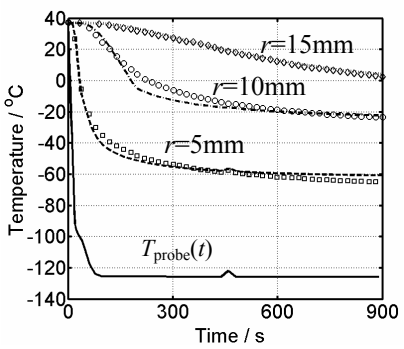

Fig. 3 Verification of the predicted thermal histories: experimental (symbols) *versus* predicted thermal histories (lines).

Note: cryosurgery of porcine kidney, the thermal properties used for simulations were selected from Rupp *et al.* (2002), and the temperature measurements were taken at three different radial locations (i.e., 5mm, 10mm, 15mm) with a depth of 10mm.

The thermal histories at three typical locations during cryosurgical process of the porcine kidney were shown in Fig. 3, the lines were the predicted results by FED with the thermal properties and the symbols were the experimental measurements selected from Rupp *et al.* (2002). As can be seen, the predictions agreed well with the measurements. The thermal results of our method were reliable.

III. RESULTS

A. Temperature and thermal gradients of the target points

From Fig. 4, for both systems the typical points (points M and N, as shown in Fig. 1) have a similar thermal history, but system CH can supply the target tissue a much lower minimal temperature and a much faster heating rate.

It can be seen from Fig. 5, the thermal gradient histories of the typical points (points M and N, as shown in Fig. 1) are all similar in tendency for both systems: i) during the freezing process, points M or N will experience a large thermal gradient peak; ii) during the following holding process, the thermal gradient tends to be steady; iii) during the warming process, the thermal gradient will diminish rapidly, then it will experience another smaller peak once the phase change begins; iv) during the second holding process, once the phase change of the tissue is completed, the thermal gradient tends to be a smaller value. During the freezing process, the thermal gradient peaks of both systems are very close to each other, but during the following holding process, the thermal gradient of System CH is apparently larger than that of System Endocare. Although all the thermal gradient peaks during the warming process along with the thawing of the iceball will appear at about -8°C, they are diverse in the absolute values. The value of point M for system CH tends to be the smallest one.

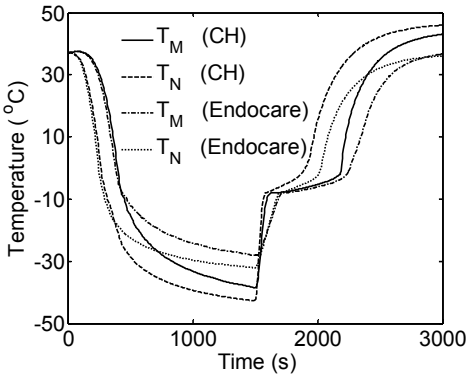

Fig. 4 Temperature histories of the typical points M and N during the cryosurgery process.

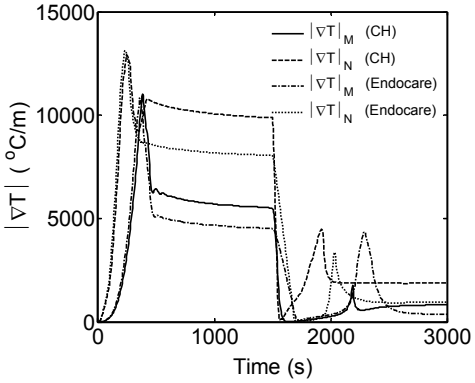

Fig 5. Thermal gradient histories of points M and N during the cryosurgery process.

B. Thermal distributions along path-*x* and path-*y*

Figures 6~9 show the temperature distributions of Path-*x* and Path-*y* (the typical paths as shown in Fig. 1) at 8 typical times (300s, during the cooling process; 1000s, during the first holding process; 1500s, at the end of the first holding process; 1530s and 1535s, during the warming process; 1562s, at the end of the warming process; 2000 and 3000s, during the second holding process) for System CH, and 10 typical times (300s, during the cooling process; 1000s, during the first holding process; 1500s, at the end of the first holding process; 1550, 1600, and 1650s, during the warming process; 1718s, at the end of the warming process; 2000, 2400, and 3000s, during the second holding process) for System Endocare.

From these 4 figs, it can be seen, i) no matter for the cooling or the warming process, once the iceball (frozen tissues) exists, the temperature-varying regions are confined in the frozen tissues, that is, the temperature nearly kept unvarying outside the iceball; ii) System CH can supply the frozen tissues a lower minimal temperature (about -175°C near the cryoprobe), and a much faster warming rate (about 240°C/min near the cryoprobe); iii) at 1562s, the thermal distributions along path-*x* and path-*y* are both "U" shaped for System CH, and at the certain ranges of path-*x* or path-*y*, the curves are nearly horizontal; iv) although all the curves of both

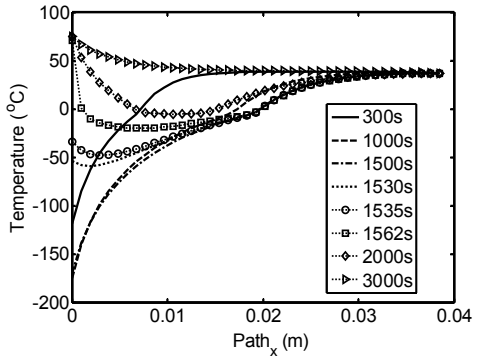

Fig. 6 Temperature distributions along Path-*x* at 8 typical times (System CH).

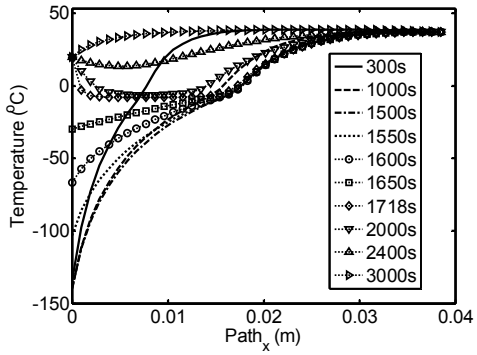

Fig. 7 Temperature distributions along Path-*x* at 10 typical times (System Endocare).

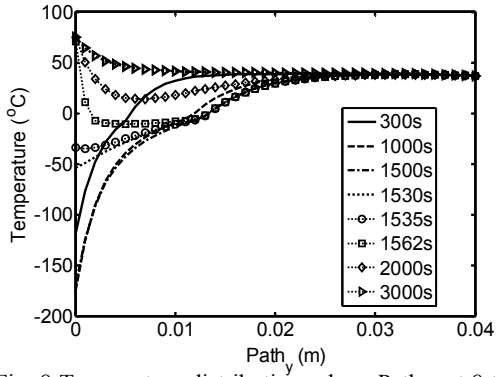

Fig. 8 Temperature distributions along Path-*y* at 8 typical times (System CH).

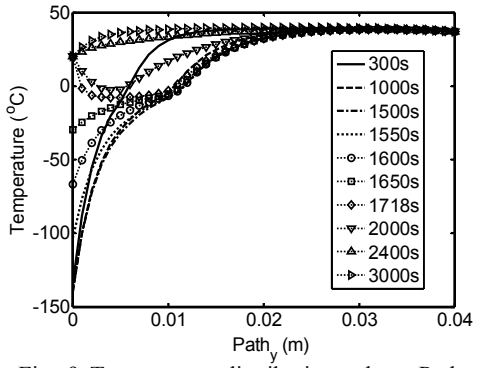

Fig. 9 Temperature distributions along Path-*y* at 10 typical times (System Endocare).

systems have similar tendency along time, the temperature acutely varying region of System CH is much wider than that of System Endocare; v) due to the heating feature of System CH, the temperature of the tissue around the probe even exceeds 50°C after 1562s, while the frozen shell still exists.

C. The propagations of the freezing fronts and the critical isothermal surfaces in *x*-direction

The propagations of the freezing fronts and the critical isothermal surfaces (-1°C , -40°C, 50°C) at the typical times are shown in Fig. 10.

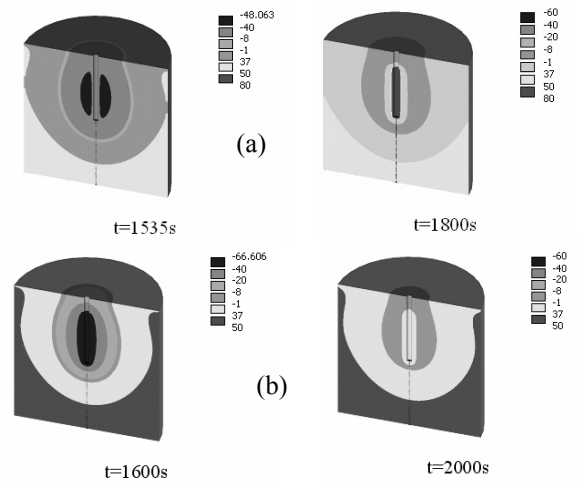

Fig. 10 The longitudinal cross-sectional temperature contours of the tumor tissue, (a) 1535 and 1800s for the new system; (b) 1600 and 2000s for the Endocare system.

From such figures as Fig. 10, the development of the freezing fronts (-1°C), the -40°C and the 50°C isothermal surfaces in *x*-direction are available. And they are shown in Figs. 11 and 12 for System CH and System Endocare separately. From the curves, it can be seen: i) during the freezing and the first holding processes, the iceball and the -40°C isothermal surface keep growing, both of them reach their maximums at 1500s ; ii) the maximal radius of the iceball is about 22mm for System CH, while it is only 19mm for System Endocare; iii) the maximal radius of the -40°C isothermal surface is about 11mm for System CH, while it is only 9mm for System Endocare; iv) for either system, a second freezing front (the inner one) will appear shortly after the warming process, that is, a hollow frozen ball will appear, and then the two freezing fronts (the inner and the outer ones) will move together, until they meet and the frozen region dissolves completely; v) the -40°C isothermal surface (the outer one) will also be reduced along with the warming process for both systems, a second -40°C isothermal surface (the inner one) will appear for System CH, and the behaviors of the two -40°C isothermal surfaces are the same to that of the above mentioned two freezing fronts, but the inner -40°C isothermal surface will not appear for System Endocare; vi) due to the new heating feature of System CH, a hot ball will appear and the 50°C isothermal surface will keep growing

during the heating process, the maximal radius of the ball in *x*-direction is about 7mm at 3000s.

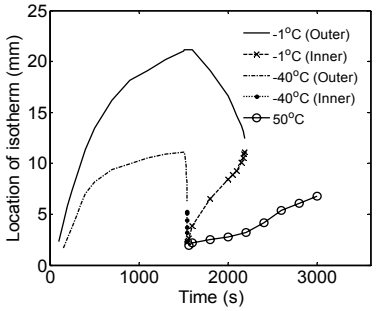

Fig. 11 Isothermal surface propagation in *x*-direction (-1°C , -40°C and 50°C, System CH).

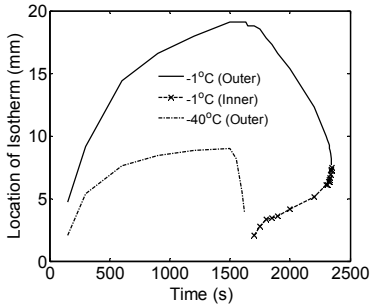

Fig. 12 Isothermal surface propagation in *x*-direction (-1 and -40°C, System Endocare).

D. The thermal distribution when the iceball reaches its maximal dimension

The longitudinal cross-sectional temperature contours of the tumor tissues for both systems at 1500s are shown in Fig. 13. As can be seen that the thermal distributions of both systems are completely similar, the only difference is that the corresponding isothermal surface of System CH is larger than that of System Endocare. The iceball of the former is apparently larger than that of the latter. In a word, System CH has a much higher freezing efficiency.

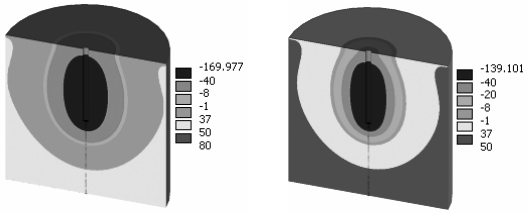

Fig. 13 The longitudinal cross-sectional temperature contours of the tumor tissue at 1500s, (a) System CH and (b) System Endocare.

IV. DISSCUSSION

A. Thermal properties

The tumor and the normal tissues were assumed to have the same thermal properties due to the lack of experimental data to distinguish them over the studied temperature range (the only known parameter for one tumor tissue is the metabolic heat generation, 33.8kW·m^{-3}). Thermal conductivity was regard as a constant for all frozen regions, and regarded as another constant for all unfrozen regions, which varied linearly with temperature during phase transformation. The latent heat was also regarded to be released linearly with temperature during phase transformation. Although the thermal dependent thermal conductivities and enthalpies of biological tissues could be measured experimentally, the valuable data are still scarce, especially at subzero temperatures. So these parameters need to be experimentally determined to make the model more accurate.

B. The blood perfusion and the metabolic heat

During the real cryosurgery process, the anisotropic blood supply network (especially, when large blood vessel across the target tissue) may make this problem more complex, so the examination of the target tumor tissue in advance is of prime importance in optimizing the cryosurgery, for it can supply the surgeon with more detailed information to set up a more accurate model on the target tissue. The finite element framework presented here are completely applicable for these non-irregular shaped tumor tissues with highly nonlinear thermal properties.

It also should be pointed out that the local blood supply network may partly be destroyed (such as vasoconstriction, vasodilation, destroy or aberrance of capillary vessel, and hyperemia of tissue) during the freeze-thaw cycles, so if this framework is used to optimize cryosurgical process, these factors must be fully considered.

V. CONCLUSIONS

In this research, the heat transfer problems during the cryosurgical processes with System CH and System Endocare were comparatively studied by using the FED.

Due to the strong heating feature of System CH, it can provide two critical isothermal surfaces, one is for the freezing injury, and the other is for the burn threshold. The simulations indicate that System CH can provide double curative effect on the tumor tissues.

ACKNOWLEDGEMENTS

This work was supported by the National Natural Science Foundation of China (No. 50506029), Anhui Provincial Natural Science Foundation (No. 070413099) and the China Postdoctoral Science Foundation (No. 2004036141).

REFERENCES

Baust, J.G. and A.A. Gage, "Progress toward optimization of cryosurgery," *Technol. Cancer Res. Treat.*, **3**, 95-101 (2004).

Deng, Z.S. and J. Liu, "Modeling of multidimensional freezing problem during cryosurgery by the dual reciprocity boundary element method," *Engineering Analysis with Boundary Elements*, **28**, 97-108 (2004a).

Deng, Z.S. and J. Liu, "Numerical simulation of 3-D freezing and heating problems for combined cryo-

surgery and hyperthermia therapy," *Numer. Heat Tr. A-Appl.*, 46, 587-611 (2004b).

Deng, Z.S. and J. Liu, "Numerical simulation of selective freezing of target biological tissues following injection of solutions with specific thermal properties," *Cryobiology*, **50**, 183-192 (2005).

Gage, A.A., J.A. Caruana and M. Montes, "Critical temperature for skin necrosis in experimental cryosurgery," *Cryobiology*, **19**, 273-282 (1982).

Gage, A.A., K. Guest, M. Montes, J.A. Caruana and D.A. Whalen, "Effect of varying freezing and thawing rates in experimental cryosurgery," *Cryobiology*, **22**, 175-82 (1985).

Gage, A.A., "Cryosurgery in the treatment of cancer," *Surg. Gynecol. Obstet.*, **174**, 73-92 (1992).

Gage, A.A. and J. Baust, "Mechanisms of tissue injury in cryosurgery," *Cryobiology*, **37**, 171-186 (1998).

Gage, A.A., "Selective cryotherapy," *Cell Preservation Technology*, **2**, 3-14 (2004).

Hamer, F.C., G. Horne, E.H. Pease, P.L. Matson and B.A. Lieberman, "The quarantine of fertilized donated oocytes," *Hum. Reprod.*, **10**, 1194-1196 (1995).

Hua, T.C. and H.S. Ren, *Cryobiomedical Techniques*, Science Press, Beijing, P.R. China (1994).

Lee, A.S.J., "Freezing probe for the treatment of tissue, especially in neurosurgery," *US Patent*, 3,298,371 (1967).

Liu, J., Y.X. Zhou and T.H. Yu, "Tumor treatment equipment based on alternatively ventilating with high and low temperature medium," *China Patent*, 01268378.7 (2001).

Liu, J., Y.X. Zhou, T.H. Yu, L. Gui, Z.S. Deng and Y.G. Lv, "Minimally invasive probe system capable of performing both cryosurgery and hyperthermia treatment on target tumor in deep tissues," *Minim. Invasiv. Ther.*, **13**, 47-57 (2004).

Mazur, P., S.P. Leibo and E.H Chu, "A two-factor hypothesis of freezing injury. Evidence from Chinese hamster tissue-culture cells," *Exp. Cell Res.*, **71**, 345-55 (1972).

Miller, R.H. and P. Mazur. "Survival of frozen-thawed human red cells as a function of cooling and warming velocities," *Cryobiology*, **13**, 404-414 (1976).

Pennes, H.H., "Analysis of tissue and arterial blood temperatures in the resting human forearm," *J. Appl. Physiol.*, **1**, 93-122 (1948).

Rabin, Y. and A. Shitzer, "Numerical solution of the multidimensional freezing problem during cryosurgery," *J. Biomech. Eng.*, **120**, 32-37 (1998).

Rabin, Y. and T.F. Stahovich, "Cryoheater as a means of cryosurgery control," *Phys. Med. Biol.*, **48**, 619-632 (2003).

Rand, R.W., R.P. Rand, F.A. Eggerding, M. Field, L. Denbesten, W. King and S. Camici, "Cryolumpectomy for breast cancer: an experimental study," *Cryobiology*, **22**, 307-318 (1985).

Rewcastle, J.C., G.A. Sandison, L.J. Hahn, J.C. Saliken, J.G. McKinnon and B.J. Donnelly, "A model for the time-dependent thermal distribution within an iceball surrounding a cryoprobe," *Phys. Med. Biol.*, **43**, 3519-3534 (1998).

Rupp, C.C., N.E. Hoffmann, F.R. Schmidlin, D.J. Swanlund, J. C. Bischof and J.E. Coad, "Cryosurgical changes in the porcine kidney: histologic analysis with thermal history correlation," *Cryobiology*, **45**, 167-182 (2002).

Saliken, J.C., J.G. McKinnon and R. Gray, "Computed tomography for cryotherapy monitoring," *Am. J. Radiol.*, **166**, 853-855 (1996).

Sandison, G.A., M.P. Loye, J.C. Rewcastle, L.J. Hahn, J.C. Saliken, J.G. McKinnon and B.J. Donnelly, "X-ray CT monitoring of iceball growth and thermal distribution during cryosurgery," *Phys. Med. Biol.*, **43**, 3309-3324 (1998).

Shitzer, A. and R.C. Eberhart, *Heat Transfer in Biology and Medicine*, Plenum Press, New York (1985).

Smith, J.J. and J. Fraser, "An estimation of tissue damage and thermal history in the cryolesion," *Cryobiology*, **11**, 139-147 (1974).

Tackenberg, J.N., "Cryolumpectomy: another option for breast cancer," *Nursing*, **20**, 32J-34J (1990).

Wessling, F.C. and P.L. Blackshear, "The thermal properties of human blood during freezing process," *ASME Journal of Heat Transfer*, **95**, 246-249 (1973).

Zhang, J., T.C. Hua and E.T. Chen, "Experimental measurement and theoretical analyses of the freezing-thawing processes around a probe," *CryoLetters*, **21**, 245-254 (2000).

Zhang, Y.T. and J. Liu, "Study on thermal stress in living tissues during cryosurgical rewarming (in Chinese)," *Space Medicine & Medical Engineering*, **15**, 291-295 (2002).

Zhang, J.Y., G.A. Sandison, J.Y. Murthy and L.X. Xu, "Numerical simulation for heat transfer in prostate cancer cryosurgery," *Journal of Biomechanical Engineering-Transactions of the ASME*, **127**, 279-294 (2005).

Zhao, G., X.F. Bai, D.W. Luo and D.Y. Gao, "Modeling the heat transfer problem for the novel combined cryosurgery and hyperthermia system," *CryoLetters*, **27**, 115-126 (2006a).

Zhao, G., D.W. Luo and D.Y. Gao, "Universal model for intracellular ice formation and its growth," *AIChE Journal*, **52**, 2596-2606 (2006b).

Zhao, G., H.F. Zhang, X.J. Guo, D.W. Luo and D.Y. Gao, "Effect of blood flow and metabolism on multidimensional heat transfer during cryosurgery," *Med. Eng. Phys.*, **29**, 205-215(2007).

Received: August 11, 2006.
Accepted: February 7, 2007.
Recommended by Subject Editor Walter Ambrosini.